JACS
JOURNAL OF THE AMERICAN CHEMICAL SOCIETY

Communication

pubs.acs.org/JACS

One-Pot Synthesis of Cubic $PtCu_3$ Nanocages with Enhanced Electrocatalytic Activity for the Methanol Oxidation Reaction

Bao Yu Xia, Hao Bin Wu, Xin Wang, and Xiong Wen (David) Lou*

School of Chemical and Biomedical Engineering, Nanyang Technological University, 70 Nanyang Drive, Singapore 637457, Singapore

Supporting Information

ABSTRACT: Noble metals such as platinum (Pt) are widely used as catalysts in fuel cells and other heterogeneous catalytic processes. However, there is an urgent need to develop substitutes for pure Pt catalysts to reduce the overall use of precious Pt and at the same time to enhance poisoning resistance. A promising strategy is to design Pt based bi- or trimetallic nanostructures because their unique structures and compositions would enhance their catalytic performance. In this study, we report the synthesis, characterization, and electrochemical evaluation of cubic intermetallic $PtCu_3$ nanocages. The influential effects of several important experimental parameters on the final products have been explored through systematic studies on the growth of $PtCu_3$ nanocages. Relative to the current commercial Pt electrocatalyst, these $PtCu_3$ nanocages possess a more accessible surface area and a unique hollow structure, which contribute to improved electrocatalytic activity in the methanol oxidation reaction.

Noble metals like Pt are widely used as the effective catalyst component in heterogeneous catalytic processes, such as CO/NO_x oxidation, petroleum cracking, and fuel cells.[1,2] It is generally known that the size, shape, composition, and structure of Pt-based catalysts are important parameters that determine the catalytic activity.[3] Pt nanomaterials with unique morphologies have attracted considerable interest because of their intriguing properties and applications in the past decades. At present, shape-controlled synthesis of Pt nanocrystals has been extensively studied to improve the catalytic activity through modification of the surface atomic arrangement of particles.[4] Nevertheless, considering the limited resource of Pt on earth, there is an urgent need to develop substitutes for pure Pt catalysts to reduce the overall use of Pt and enhance poisoning resistance at the same time.[5,6]

Because of their high surface to volume ratio and large void space, hollow structured Pt nanomaterials, including nanocages,[7−9] hollow nanospheres,[10,11] and nanoboxes,[12−16] have received tremendous attention as electrocatalysts.[17] Moreover, as high activity catalysts, Pt based bimetallic nanocrystals would not only reduce the consumption of Pt but also bring enhanced activities to catalyze multistep processes in which each metal component participates mainly in one step.[18] Therefore, another important route for greatly improving the activity and stability of Pt catalysts is to design Pt based bi- or trimetallic nanostructures with controlled architectures,[19] which have received more attention recently as low-cost catalysts.[20] In particular, Pt-containing alloy nanocrystals such as PtNi,[21,22] PtCo,[23−25] PtSn,[26,27] and PtCu[28−30] have attracted increasing interest as electrocatalysts. Recent reports indicate that the electrocatalytic activities of these Pt based bimetallic nanocrystals are superior to those of pure Pt counterparts.[31] Such alloy nanocrystals possess not only large surface areas but also unique structural properties.[19,32−34] Therefore, it is of great importance to synthesize advanced electrocatalysts that will not only reduce the Pt loading amount but also increase the activity and stability of Pt based electrocatalysts.[35,36]

Herein, we report an efficient synthesis of novel intermetallic $PtCu_3$ nanocages and their attractive electrocatalytic activity toward the methanol oxidation reaction. The influence of several important synthesis parameters on the final products is also systematically investigated. Relative to the current Pt nanoparticle electrocatalysts, the as-synthesized Cu-rich $PtCu_3$ nanocages exhibit improved electrocatalytic activity presumably because of some possible synergetic effect of the two metallic components.

In a typical synthesis of $PtCu_3$ nanocages, chloroplatinic acid hexahydrate ($H_2PtCl_6{\cdot}6H_2O$), copper(II) acetylacetonate [Cu(acac)$_2$], and cetyltrimethylammonium bromide (CTAB) are dissolved in oleylamine (OAm). The resultant homogeneous solution is then solvothermally treated in a Teflon-lined stainless steel autoclave at 170 °C for 24 h. A typical transmission electron microscope (TEM) image shows that the sample consists of nanocages with an edge size of ~20 nm, and the morphological yield is greater than 95% (Figure 1a). Further examination (Figure 1b) reveals that these nanocages possess an obvious hollow cubic structure (the model of a cubic nanocage structure is displayed in the inset of Figure 1b), though some particles appear like hexagonal stars at first glance due to the particular orientation. The selected-area electron diffraction (SAED) pattern of the nanocages (Figure 1, c1) indicates the high crystallinity of these nanocages. The cubic morphology and hollow structure are further elucidated by different nanocages shown in Figure 1 (c2−c4). It can be seen that the nanostructures have clear edges and corners. Figure 1d shows more free-standing nanocages with different orientations, which again confirms the hollow cubic structure.

The as-prepared product is also characterized by field-emission scanning electron microscopy (FESEM). As shown in Figure S1 (see Supporting Information (SI)), the product

Received: May 28, 2012
Published: August 16, 2012

   dx.doi.org/10.1021/ja3051662 | J. Am. Chem. Soc. 2012, 134, 13934−13937

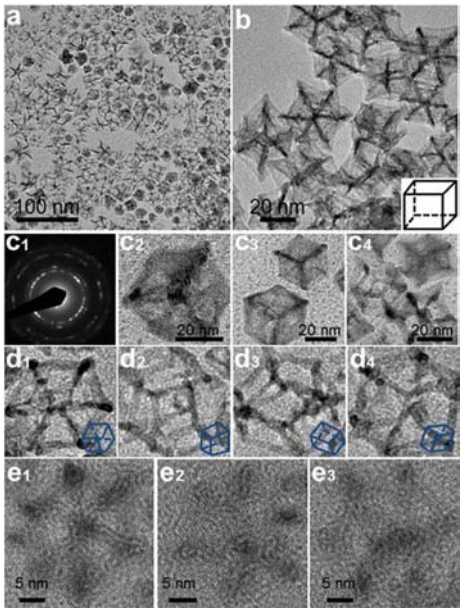

Figure 1. TEM (a, b, c2−c4, d1−d4) and HRTEM (e1−e3) images of $PtCu_3$ nanocages: (a) low magnification, (b) high magnification, inset of (b) is the model of a cubic nanocage. (c1) Selected-area electron diffraction (SAED) pattern; (c2−c4) nanocages. (d1−d4) Nanocages with different orientations; the insets are the corresponding crystal model.

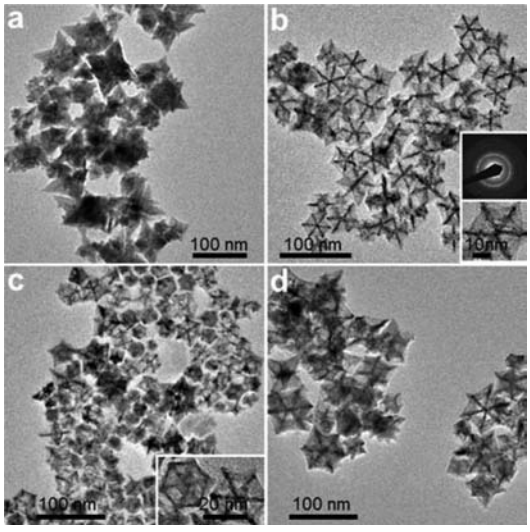

Figure 2. TEM images of products obtained with different reaction durations: (a) 12 h; (b) 20 h; (c) 28 h; and (d) 36 h.

mainly consists of uniform cubic nanoparticles. The nanocage composition has been investigated by energy dispersive X-ray (EDX) spectroscopy equipped with FESEM and TEM. The consistent results obtained suggest a Pt/Cu molar ratio of ∼1:3 (Figure S1c; see SI). A powder X-ray diffraction (XRD) technique is employed to identify the crystalline structure of as-prepared products. The XRD pattern (Figure S2; see SI) of the nanocages displays characteristic peaks that are in agreement with that of the standard $PtCu_3$ pattern (JCPDS No. 35-1358). Moreover, no obvious peaks from either Pt or Cu are detected, thus confirming the purity of the intermetallic $PtCu_3$ phase. As shown in Figure 1 (e1−e3), high-resolution (HR) TEM images further reveal the hollow cubic structure of these $PtCu_3$ nanocages and clear lattice fringes with an interplanar distance of approximately 0.22 nm. Furthermore, the elemental mapping analysis (Figure S3; see SI) shows the uniform distribution of both Pt and Cu elements.

To better understand the formation process of these $PtCu_3$ nanocages, the intermediate nanocrystals produced at different reaction durations are investigated by TEM. Figure 2 shows the morphological evolution of the particles with the reaction time. The nanoparticles collected after reaction for 12 h possess a uniform and concave solid morphology with sizes in the range of 20−50 nm, while the hollow nanocage structure is hardly observed (Figure 2a). With the increasing reaction time, the structure of these nanocrystals continues to evolve. The cage structure can be clearly observed in the products obtained with reaction durations of 20 and 28 h (Figure 2b and c), and there is no further pronounced change in structure for the product obtained with a reaction time of 36 h (Figure 2d). It has been reported that oleylamine can serve simultaneously as the solvent, reducing agent, and stabilizer for the synthesis of metal nanocrystals.[37] Additionally, CTAB also plays an important role in the formation of the nanocage structure. In the absence of CTAB, mixed polyhedra of Pt−Cu nanocrystals are obtained (Figure S4a; see SI). When the amount of CTAB is increased from 0 to 50 mg, the cage structure gradually appears and the nanocrystals are dispersed more uniformly (Figure S4b and c). We postulate that the presence of CTAB would probably affect the reduction rates of Pt and Cu species; thus Cu nanocrystals are first formed although the standard reduction potential (E) for Cu^{II}/Cu (0.34 V) is more negative than that of the Pt^{II}/Pt pair (1.18 V). The following galvanic replacement of Cu nanocrystals with Pt species in the solution finally leads to the formation of $PtCu_3$ hollow nanocages.[35] However, when the amount of CTAB is further increased to 150 mg, nanocages would be coated by the excessive CTAB, leading to aggregation (Figure S4d). Thus, it is suggested that an appropriate amount of CTAB as a structure directing and stabilizing agent can favor the formation and dispersion of $PtCu_3$ nanocages.[4,37,38]

These Cu-rich intermetallic $PtCu_3$ nanocages would be of great interest as electrocatalysts.[39] It is suggested that the selective electrochemical dissolution of Cu is the key process in the formation of the active electrocatalyst.[40] As shown in Figure 3a, the second-cycle cyclic voltammogram (CV) curve shows no characteristic H-ad/desorption peaks (−0.24 - 0.1 V), which is due to the complete Cu surface segregation in Cu-rich Pt−Cu alloys (0.2 V).[40] In the fifth cycle CV curve, the intensity of the Cu dissolution peaks decreases further, while the H-ad/desorption features gradually emerge. After ∼50 cycles, the features associated with dissolution of Cu are completely absent, giving rise to a stable Pt-like CV profile. Subsequent cycling up to 200 cycles results in little change in the CV profile while the cubic nanocage structure is generally retained (Figure S5; see SI) and the Pt/Cu atomic ratio changes to ∼3:1 (Figure S6; see SI). This observation suggests that the active Pt−Cu electrocatalyst is indeed derived through the initial dealloying process.[41] This electrochemical dealloying process would endow $PtCu_3$ nanocages with some advantageous material characteristics such as large surface area and atomic rearrangement which are desirable for their electrocatalytic activity.[40,42] The electrochemical active surface area (ECSA) can be calculated by integrating the charge passing the electrode during the hydrogen adsorption/desorption process after the correction for the double layer formation. The charge required to oxidize a hydrogen monolayer is 0.21 mC cm^{-2},

dx.doi.org/10.1021/ja3051662 | J. Am. Chem. Soc. 2012, 134, 13934−13937

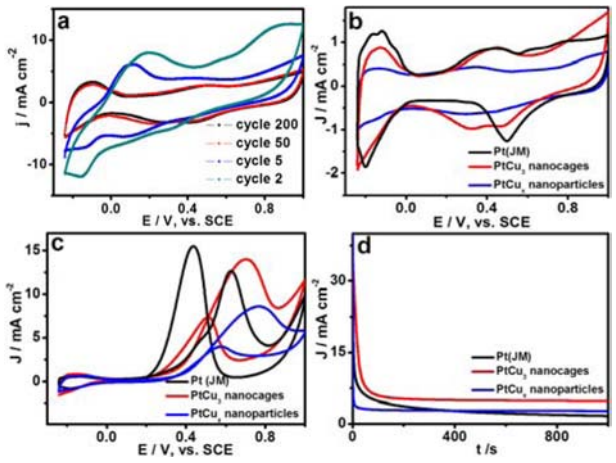

Figure 3. (a) Cyclic voltammetric (CV) profiles of $PtCu_3$ cubic nanocages at 100 mV s^{-1}. (b) CV profiles of $PtCu_3$ cubic nanocages, $PtCu_x$ solid nanoparticles, and Pt(JM) in a 0.1 M $HClO_4$ solution (20 mV s^{-1}). (c) CV and (d) chromoamperometric (CA) results of MeOH oxidation on $PtCu_3$ nanocages, $PtCu_x$ solid nanoparticles, and Pt(JM) in a 0.1 M $HClO_4$ + 1 M MeOH solution (20 mV s^{-1}). CA curves were recorded at 0.75 V vs SCE.

corresponding to a surface density of 1.3×10^{15} Pt atoms per cm^2.[43] As shown in Figure 3b, the specific ECSA of $PtCu_3$ is 35.7 m^2 g^{-1}, which is ~73% of that of the commercial Pt electrocatalyst (48.6 m^2 g^{-1}; JM, 20 wt % Pt, Pt particle size ≈ 3 nm; Figure S7; see SI) and 3 times that of $PtCu_x$ solid nanoparticles ($x \approx 9$; Figures S8 and S9; see SI) shown in Figure 2a after the dealloying process (12.1 m^2 g^{-1}; Figures S10 and S11; see SI). The lower ECSA for the $PtCu_3$ electrocatalyst is most likely due to the large nanoparticle size, surface coating by organic species and/or some aggregation formed in the electrochemical process.

Next, we investigate the catalytic activity of the $PtCu_3$ nanocages toward the methanol oxidation. A CV profile of $PtCu_3$ in a 0.1 M $HClO_4$/1 M methanol solution is shown in Figure 3c. For comparison, CVs of $PtCu_x$ nanoparticles and the JM commercial Pt electrocatalyst are also included. It is clear that the methanol oxidation current density of $PtCu_3$ nanocages (14.1 mA cm^{-2}) is higher than that of $PtCu_x$ nanoparticles (8.4 mA cm^{-2}) and the commercial Pt electrocatalyst (12.8 mA cm^{-2}). Moreover, the $PtCu_3$ nanocages exhibit a much higher I_f/I_b (in which I_f and I_b are the forward and backward current densities, respectively) ratio compared with the commercial Pt electrocatalyst (1.93 vs 0.82). This observation implies that methanol molecules can be more effectively oxidized on the $PtCu_3$ nanocages during the forward potential scan, generating relatively less poisoning species as compared to the commercial Pt electrocatalyst.[28] The higher methanol oxidation current density on $PtCu_3$ nanocages is further confirmed by the chronoamperometric (CA) measurements performed at 0.75 V for 1000 s (Figure 3d). CA curves indicate that the current density of $PtCu_3$ is higher than that of $PtCu_x$ nanoparticles and the commercial Pt electrocatalyst for the entire time course, which further verifies that the $PtCu_3$ nanocages exhibit better electrocatalytic performance in the methanol oxidation reaction (MOR). The higher electrocatalytic activity of $PtCu_3$ nanocages might be related to the unique nanocage structure and the possible synergetic effect between Pt and Cu.[35]

In summary, novel cubic $PtCu_3$ nanocages have been prepared by a one-pot synthesis method in an organic solution system. A galvanic replacement mechanism between preformed Cu nanocrystals and Pt species is proposed to explain the formation of these novel nanocages. The as-prepared $PtCu_3$ nanocages exhibit enhanced electrocatalytic activity in the methanol oxidation reaction compared with solid $PtCu_x$ nanoparticles and a commercial single-component Pt electrocatalyst. This enhanced performance toward the methanol oxidation reaction could be attributed to the unique structure and possible synergetic effect of Pt and Cu components. Our study suggests that advanced electrocatalysts can be developed by engineering the structure and composition of the nanocatalysts.

■ ASSOCIATED CONTENT

Supporting Information

Detailed experimental procedure, additional FESEM and TEM images, XRD patterns, EDX results, and CV profiles. This material is available free of charge via the Internet at http://pubs.acs.org.

■ AUTHOR INFORMATION

Corresponding Author

xwlou@ntu.edu.sg

Notes

The authors declare no competing financial interest.

■ REFERENCES

(1) Ertl, G.; Knözinger, H.; Weitkamp, J. *Handbook of Heterogeneous Catalysis*; VCH: Weinheim, 1997.
(2) Zhou, S. H.; Varughese, B.; Eichhorn, B.; Jackson, G.; McIlwrath, K. *Angew. Chem., Int. Ed.* **2005**, *44*, 4539.
(3) Zhou, K. B.; Li, Y. D. *Angew. Chem., Int. Ed.* **2012**, *51*, 602.
(4) Sau, T. K.; Rogach, A. L. *Adv. Mater.* **2010**, *22*, 1781.
(5) Guo, S. J.; Wang, E. K. *Nano Today* **2011**, *6*, 240.
(6) Stephens, I. E. L.; Chorkendorff, I. *Angew. Chem., Int. Ed.* **2011**, *50*, 1476.
(7) Song, Y. J.; Garcia, R. M.; Dorin, R. M.; Wang, H. R.; Qiu, Y.; Shelnutt, J. A. *Angew. Chem., Int. Ed.* **2006**, *45*, 8126.
(8) Yamauchi, Y.; Sugiyama, A.; Morimoto, R.; Takai, A.; Kuroda, K. *Angew. Chem., Int. Ed.* **2008**, *47*, 5371.
(9) Hong, J. W.; Kang, S. W.; Choi, B.-S.; Kim, D.; Lee, S. B.; Han, S. W. *ACS Nano* **2012**, *6*, 2410.
(10) Liang, H. P.; Zhang, H. M.; Hu, J. S.; Guo, Y. G.; Wan, L. J.; Bai, C. L. *Angew. Chem., Int. Ed.* **2004**, *43*, 1540.
(11) Snyder, J.; McCue, I.; Livi, K.; Erlebacher, J. *J. Am. Chem. Soc.* **2012**, *134*, 8633.
(12) Murphy, C. J. *Science* **2002**, *298*, 2139.
(13) Peng, Z. M.; You, H. J.; Wu, J. B.; Yang, H. *Nano Lett* **2010**, *10*, 1492.
(14) Chen, J. Y.; McLellan, J. M.; Siekkinen, A.; Xiong, Y. J.; Li, Z. Y.; Xia, Y. N. *J. Am. Chem. Soc.* **2006**, *128*, 14776.
(15) Lee, W. R.; Kim, M. G.; Choi, J. R.; Park, J. I.; Ko, S. J.; Oh, S. J.; Cheon, J. *J. Am. Chem. Soc.* **2005**, *127*, 16090.
(16) Xia, Y. N.; Li, W. Y.; Cobley, C. M.; Chen, J. Y.; Xia, X. H.; Zhang, Q.; Yang, M. X.; Cho, E. C.; Brown, P. K. *Acc. Chem. Res.* **2011**, *44*, 914.
(17) Yin, Y. D.; Rioux, R. M.; Erdonmez, C. K.; Hughes, S.; Somorjai, G. A.; Alivisatos, A. P. *Science* **2004**, *304*, 711.
(18) Stamenkovic, V. R.; Mun, B. S.; Arenz, M.; Mayrhofer, K. J. J.; Lucas, C. A.; Wang, G. F.; Ross, P. N.; Markovic, N. M. *Nat. Mater.* **2007**, *6*, 241.
(19) Lim, B.; Yu, T. Y.; Xia, Y. N. *Angew. Chem., Int. Ed.* **2010**, *49*, 9819.
(20) Mazumder, V.; Lee, Y.; Sun, S. H. *Adv. Funct. Mater.* **2010**, *20*, 1224.

(21) Stamenkovic, V. R.; Fowler, B.; Mun, B. S.; Wang, G. F.; Ross, P. N.; Lucas, C. A.; Markovic, N. M. *Science* **2007**, *315*, 493.
(22) Zhang, J.; Yang, H. Z.; Fang, J. Y.; Zou, S. Z. *Nano Lett* **2010**, *10*, 638.
(23) Chen, G.; Xia, D. G.; Nie, Z. R.; Wang, Z. Y.; Wang, L.; Zhang, L.; Zhang, J. J. *Chem. Mater.* **2007**, *19*, 1840.
(24) Yang, H. Z.; Zhang, J.; Sun, K.; Zou, S. Z.; Fang, J. Y. *Angew. Chem., Int. Ed.* **2010**, *49*, 6848.
(25) Choi, S. I.; Choi, R.; Han, S. W.; Park, J. T. *Chem. Commun.* **2010**, *46*, 4950.
(26) Liu, Y.; Li, D. G.; Stamenkovic, V. R.; Soled, S.; Henao, J. D.; Sun, S. H. *ACS Catal.* **2011**, *1*, 1719.
(27) Liu, Z. F.; Jackson, G. S.; Eichhorn, B. W. *Angew. Chem., Int. Ed.* **2010**, *49*, 3173.
(28) Xu, D.; Liu, Z. P.; Yang, H. Z.; Liu, Q. S.; Zhang, J.; Fang, J. Y.; Zou, S. Z.; Sun, K. *Angew. Chem., Int. Ed.* **2009**, *48*, 4217.
(29) Strasser, P.; Koh, S.; Anniyev, T.; Greeley, J.; More, K.; Yu, C. F.; Liu, Z. C.; Kaya, S.; Nordlund, D.; Ogasawara, H.; Toney, M. F.; Nilsson, A. *Nat. Chem.* **2010**, *2*, 454.
(30) Yang, R. Z.; Leisch, J.; Strasser, P.; Toney, M. F. *Chem. Mater.* **2010**, *22*, 4712.
(31) Gupta, G.; Slanac, D. A.; Kumar, P.; Wiggins-Camacho, J. D.; Wang, X. Q.; Swinnea, S.; More, K. L.; Dai, S.; Stevenson, K. J.; Johnston, K. P. *Chem. Mater.* **2009**, *21*, 4515.
(32) Sau, T. K.; Rogach, A. L.; Jackel, F.; Klar, T. A.; Feldmann, J. *Adv. Mater.* **2010**, *22*, 1805.
(33) Ding, Y.; Chen, M.; Erlebacher, J. *J. Am. Chem. Soc.* **2004**, *126*, 6876.
(34) Snyder, J.; Fujita, T.; Chen, M. W.; Erlebacher, J. *Nat. Mater.* **2010**, *9*, 904.
(35) Wang, D. S.; Li, Y. D. *Adv. Mater.* **2011**, *23*, 1044.
(36) Huang, X. Q.; Zhang, H. H.; Guo, C. Y.; Zhou, Z. Y.; Zheng, N. F. *Angew. Chem., Int. Ed.* **2009**, *48*, 4808.
(37) Xu, Z.; Shen, C.; Hou, Y.; Gao, H.; Sun, S. *Chem. Mater.* **2009**, *21*, 1778.
(38) Jin, R. C.; Cao, Y. W.; Mirkin, C. A.; Kelly, K. L.; Schatz, G. C.; Zheng, J. G. *Science* **2001**, *294*, 1901.
(39) Mahmoud, M. A.; Saira, F.; El-Sayed, M. A. *Nano Lett.* **2010**, *10*, 3764.
(40) Koh, S.; Strasser, P. *J. Am. Chem. Soc.* **2007**, *129*, 12624.
(41) Chen, S.; Ferreira, P. J.; Sheng, W. C.; Yabuuchi, N.; Allard, L. F.; Shao-Horn, Y. *J. Am. Chem. Soc.* **2008**, *130*, 13818.
(42) Liu, L. F.; Pippel, E. *Angew. Chem., Int. Ed.* **2011**, *50*, 2729.
(43) Lee, E. P.; Peng, Z.; Cate, D. M.; Yang, H.; Campbell, C. T.; Xia, Y. *J. Am. Chem. Soc.* **2007**, *129*, 10634.